Role of spin-orbit coupling in the physical properties of LaX_3 (X=In, P, Bi) superconductors

H. M. Tütüncü,[1,2] Ertuğrul Karaca,[2] H. Y. Uzunok,[1,2] and G. P. Srivastava[3]
[1]*Sakarya Üniversitesi, Fen-Edebiyat Fakültesi, Fizik Bölümü, 54187, Adapazarı, Turkey*
[2]*Sakarya Üniversitesi, BIMAYAM Biyomedikal, Manyetik ve Yarıiletken Malzemeler Araştırma Merkezi, 54187, Adapazarı, Turkey*
[3]*School of Physics, University of Exeter, Stocker Road, Exeter EX4 4QL, United Kingdom*

(Received 12 February 2018; revised manuscript received 20 March 2018; published 14 May 2018)

We report a comprehensive and complementary study on structural, elastic, mechanical, electronic, phonon, and electron-phonon interaction properties of LaX_3 (X = In, Pb, and Bi) using first-principles density functional calculations within the local density approximation with and without the spin-orbit coupling (SOC). The calculated lattice parameters for these intermetallic compounds with and without SOC are found to differ by less than 2% from their experimental values. The effect of SOC on the elastic, mechanical, electronic, phonon, and electron-phonon interaction properties is more profound for $LaPb_3$ and $LaBi_3$ containing heavier X elements rather than $LaIn_3$ containing lighter X element. The inclusion of SOC considerably removes the degeneracies of some bands near the Fermi level and makes some phonon branches in $LaPb_3$ and $LaBi_3$ softer and increases the strength of dominant peaks in their Eliashberg spectral functions. Thus the SOC related enhancement of their electron-phonon coupling parameter values can be related to both a softening of their phonon dispersion curves and an increase in their electron-phonon coupling matrix elements. The superconducting transition temperature with SOC is computed to be 0.69 K for $LaIn_3$, 4.23 K for $LaPb_3$, and 6.87 K for $LaBi_3$, which agree very well with the respective measured values of 0.70, 4.18, and 7.30 K.

DOI: 10.1103/PhysRevB.97.174512

I. INTRODUCTION

For several decades, REX_3 (RE = rare earth, X = Sn, In, Ga, Al, Pb, and Pd) compounds crystallizing in the $AuCu_3$ cubic structure have been the issue of countless experimental studies [1–29] because of phenomena such as magnetic moment formation, crystal field and Kondo effect, or multiaxial magnetic structures, due to their incomplete 4f bands. Several LaX_3 (X = In, Sn, Tl and Pb) compounds have been reported to display superconductivity. In particular, $LaIn_3$ and $LaPb_3$ display superconductivity at around 0.70 and 4.05 K, respectively [30,31]. Heat capacity measurements of $LaIn_3$ [32] have been used to derive its electronic specific heat coefficient γ, density of states at the Fermi level [$N(E_F)$] and Debye temperature (Θ_D). In this experimental work [32], from the experimentally obtained superconducting transition temperature (T_c), the value of electron-phonon coupling parameter (λ) for $LaIn_3$ is estimated to be 0.59, which reveals that this intermetallic compound is a conventional phonon-mediated superconductor with weak electron-phonon interaction. Similarly, in the experimental works of Toxen and co-workers [33,34], the value of λ for $LaIn_3$ is reported to be 0.44, which also confirms that the electron-phonon interaction in $LaIn_3$ is rather weak. Following these experimental studies, the experimental value of T_c for $LaPb_3$ has been reported to be 4.18 K in the work of Welsh and co-workers [35], while thermal and magnetic properties of this material have been presented in the experimental study of Canepa and co-workers [36]. The Debye temperatures of $LaIn_3$ and $LaPb_3$ are derived to be 210 and 125 K, respectively, from specific heat measurements made by Kletowski *et al.* [37]. Recently, an electron spin resonance study [38] of the $LaIn_{3-x}Sn_x$ superconducting system confirms that the T_c value of $LaIn_3$ is around 0.70 K and it exhibits an oscillatory dependence as a function of Sn substitution, reaching its largest value $T_c \approx 6.4$ K for the $LaSn_3$ end member.

On the theoretical side, the electronic and cohesive properties of $LaIn_3$ have been studied by Hackenbracht and Kübler [39] using the augmented plane-wave method (APW). From their electronic result, they have determined the value of λ to be 0.11. However, this coupling constant is much lower than its experimental value of 0.44 [33,34] and can not lend to the previously measured T_c value. The electronic properties of $LaIn_3$ have also been studied by using the linearized muffin-tin-orbital method with the atomic sphere approximation (LMTO-ASA) [40]. This theoretical work indicates that the interaction between La d and In p forms the main bonding states in this superconductor, thus suggesting that this material acts like a transition metal compound. After this theoretical work, the electronic and elastic properties of LaX_3 (X = Pb, In, and Tl) have been presented under pressure using the FP-LAPW method within the local density approximation (LDA) [41]. This theoretical work proposes that the bands near the Fermi level for these superconductors consist mostly of X p orbitals with significant contributions from La d orbitals. Abraham and co-workers [42] have also utilized the FP-LAPW method to study physical properties of these superconductors. However, their calculations have been made within the generalized gradient approximation (GGA) rather than the LDA. A comparison of these two FP-LAPW [41,42] works shows that the values of the calculated second-order elastic constants for $LaIn_3$ differ from each other within around 30%. This difference can be related to the different exchange-correlation approximations used in these FP-LAPW works [41,42].

Very recently, using a high-pressure technique, Kinjo and co-workers [43] have researched for new compounds among the aforesaid LaX_3 compound and found that $LaBi_3$ also has the $AuCu_3$-type structure with the T_c value of 7.3 K, which is larger than the T_c value for $LaPb_3$. They proposed that the difference between the $N(E_F)$ values for these two compounds is mainly responsible for their different T_c values. However, we think that it is very early to reach this conclusion since the value of λ depends mainly on the phonon properties rather than on the electronic properties of a metal [44]. Thus, in order to discover the reason behind the difference in the T_c values for different LaX_3 compounds, one has to study their phonon properties, such as phonon dispersion relations and the electron-phonon interaction parameter. Moreover, the influence of spin-orbit coupling (SOC) on their phonon properties must be considered since Heid and co-workers [45] have observed that the inclusion of this interaction softens phonon modes in Pb. Indeed, their work suggests that the softening of the phonon spectrum of Pb increases the value of λ by 44%.

With the above discussion in mind, in this study we aim to search the SOC effect on the structural, elastic, mechanical, electronic, phonon, and electron-phonon interaction properties of $LaIn_3$, $LaPb_3$, and $LaBi_3$. We present our numerical results on the structural, elastic, mechanical, and electronic properties of these compounds using the LDA of density functional theory (DFT) with and without the SOC [47,48]. In particular, the effect of SOC on the bands close to the Fermi level for all the studied superconductors is studied and discussed. Furthermore, we have carried out *ab initio* linear response calculations of phonon dispersion curves and electron-phonon interaction matrix elements. Then, these quantities are utilized to obtain the Eliashberg spectral function [47–51] for all the studied materials, from which the value of average electron-phonon coupling parameter is derived. The influence of SOC on the phonon spectrum of $LaIn_3$ is negligible due to the smaller mass of In as compared to the masses of Pb and Bi. However, with inclusion of SOC, some phonon frequencies decrease in $LaPb_3$ and $LaBi_3$, and their average electron-phonon coupling parameters increase considerably, which causes enhancement in their T_c values. Using the calculated value of the electron-phonon coupling parameter, the value of T_c is estimated to be 0.69 K for $LaIn_3$, 4.23 for $LaPb_3$, and 6.88 K for $LaBi_3$, which are consistent with the corresponding measured values of 0.70 K, 4.18 K, and 7.3 K [31,35,43]. Our results reveal that with phonon dispersions calculated with the inclusion of SOC, the superconductivity mechanism in these three superconductors can be explained very well with the traditional scheme involving electron-phonon interaction.

II. THEORY

This study has been made using the *ab initio* pseudopotential plane-wave self-consistent method, based on the density functional theory within the local-density approximation [46–48]. All calculations have been performed, with and without SOC for In, Pb, and Bi, by using the 6.1 version of QUANTUM ESPRESSO package (QEP) [46–48]. We have adopted the Ceperley-Alder [52] exchange and correlation functional with the parametrization of Perdew and Zunger [53]. The interaction of the valence electrons with ionic cores is defined by ultrasoft pseudopotentials [54,55]. For calculations without SOC, we used the scalar-relativistic Vanderbilt-type ultrasoft pseudopotential for all the elements: these being la-lda-v1.uspp.F.UPF [54,56] for La, In.pz-dn-rrkjus$_{psl}$.0.2.2.UPF [55,57] for In, Pb.pz-dn-rrkjus$_{psl}$.0.2.2.UPF [55,57] for Pb, and Bi.pz-dn-rrkjus$_{psl}$.0.2.2.UPF [55,57] for Bi. For calculations with SOC, we used the scalar-relativistic ultrasoft pseudopotential for Li, and full-relativistic ultrasoft pseudopotentials for the other elements [55,57]: In.rel-pz-dn-rrkjus$_{psl}$.0.2.2.UPF for In, Pb.rel-pz-dn-rrkjus$_{psl}$.0.2.2.UPF for Pb, and Bi.rel-pz-dn-rrkjus$_{psl}$.0.2.2.UPF for Bi. The cutoffs for the wave functions and the charge density are chosen to be 60 and 600 Ry, respectively. Self-consistency in solutions to the Kohn-Sham equations [58] is accomplished by using special $\boldsymbol{k}$ points within the irreducible Brillouin zone (IBZ). The total energy calculations have been performed with a $(8 \times 8 \times 8)$ $\boldsymbol{k}$-point mesh using the Monkhorst Pack scheme [59], while a $(24 \times 24 \times 24)$ $\boldsymbol{k}$-point mesh is considered to determine electronic properties of all the considered intermetallic compounds.

The *ab initio* pseudopotential method allows us to perform total energy calculations for arbitrary crystal structures. Thus we have applied small strains to the equilibrium lattice then obtain resulting change in the total energy, and using this information deduce the second-order elastic constants. The elastic constants are defined to be proportional to the second-order coefficient in a polynomical fit of the total energy as a function of the distortion parameter δ. The cubic lattice possesses three independent second-order elastic constants, that is, C_{11}, C_{12}, and C_{44}. Thus we need three equations to obtain them. The first equation is composed of calculating the bulk modulus (B), which is linked to the values of C_{11} and C_{12} as follows [60,61]:

$$B = \frac{C_{11} + 2C_{12}}{3}. \tag{1}$$

The B and its first-order pressure derivative B' are evaluated by fitting the calculated energy-volume (E_{tot}-V) data to Murnaghan's equation of state [62]. The next step contains a volume-conserving tetragonal strain for the determination of the tetragonal shear modulus $C_{11} - C_{12}$, which is given as [60,61]

$$\overline{\varepsilon} = \begin{pmatrix} \delta & 0 & 0 \\ 0 & \delta & 0 \\ 0 & 0 & (1+\delta)^{-2} - 1 \end{pmatrix}. \tag{2}$$

This strain provides an energy change $\Delta E = 3V_o(C_{11} - C_{12})\delta^2 + O[\delta^3]$. The final step involves the volume-conserving base-centered orthorombic strain tensor, which can be defined as [60,61]

$$\overline{\varepsilon} = \begin{pmatrix} 0 & \delta/2 & 0 \\ \delta/2 & 0 & 0 \\ 0 & 0 & \frac{\delta^2}{(4-\delta)^2} \end{pmatrix}. \tag{3}$$

This strain provides an energy change $\Delta E = \frac{1}{2}C_{44}V_o\delta^2 + O[\delta^4]$. This energy change gives us the value of C_{44} directly, while the values of C_{11} and C_{12} are computed by combining the tetragonal shear modulus with the relation for the bulk modulus

in Eq. (1). After calculating the second-order elastic constants of LaX_3, the polycrystalline elastic modulus can evaluated by using the Voigt-Reuss-Hill (VRH) approach [63–65]. Using the VRH approach [63–65], the values of shear modulus (G), Young's modulus (E), Poisson's ratio (σ), and anisotropic factor (A) are derived from the below equations:

$$G_V = \frac{C_{11} - C_{12} + 3C_{44}}{5}, \quad G_R = \frac{5C_{44}(C_{11} - C_{12})}{3(C_{11} - C_{12}) + 4C_{44}}, \tag{4}$$

$$G_H = \frac{G_V + G_R}{2}, \quad E = \frac{9BG_H}{G_H + 3B}, \tag{5}$$

$$\sigma = \frac{3B - E}{6B}, \quad A = \frac{2C_{44}}{(C_{11} - C_{12})}. \tag{6}$$

After determining shear modulus G, we are able to obtain transverse, longitudinal and mean sound velocities (V_T, V_L, and V_M) from the following equations:

$$V_T = \left(\frac{G_H}{\rho}\right)^{1/2}, \tag{7}$$

$$V_L = \left(\frac{3B + 4G_H}{3\rho}\right)^{1/2}, \tag{8}$$

$$V_m = \left[\frac{1}{3}\left(\frac{2}{V_T^3} + \frac{1}{V_L^3}\right)\right]^{-1/3}. \tag{9}$$

Finally, we can estimate the Debye temperature (Θ_D) from [66]

$$\Theta_D = \frac{h}{k}\left(\frac{3n}{4\pi}\frac{N_A\rho}{M}\right)^{1/3} V_m, \tag{10}$$

where h, k, n, N_A, ρ, and M are the Planck′s constant, Boltzmann's constant, the number of atoms in the molecule, Avogadro′s number, the mass density and the molecular weight.

Having obtained self-consistent solutions of the Kohn-Sham equations, we are able to investigate the vibrational properties of all the considered compounds within the framework of the self-consistent density functional perturbation theory [47,48]. Ten dynamical matrices have been computed for a $4 \times 4 \times 4$ $\boldsymbol{q}$-point mesh within the IBZ. Then, these dynamical matrices are Fourier-transformed to real space and thus the force constants are determined, which are utilized to calculate phonon frequencies for any chosen $\boldsymbol{q}$ points. The DFT also supplies a confident framework for implementing from first principles the Migdal-Eliashberg approach for obtaining the superconducting properties of crystals. The major quantity of this approach is the Eliashberg spectral function [$\alpha^2F(\omega)$] [47–51], which can be identified in terms of the phonon linewidth $\gamma_{\boldsymbol{q}j}$ of mode j at wave vector $\boldsymbol{q}$ by

$$\alpha^2F(\omega) = \frac{1}{2\pi N(E_F)} \sum_{\mathbf{q}j} \frac{\gamma_{\mathbf{q}j}}{\hbar\omega_{\mathbf{q}j}} \delta(\omega - \omega_{\mathbf{q}j}), \tag{11}$$

where $\omega_{\boldsymbol{q}j}$ is the phonon frequency and $N(E_F)$ presents the electronic density of states per atom and spin at the Fermi level. $\gamma_{\boldsymbol{q}j}$ originating from electron-phonon interaction [47–51] can be given by

$$\gamma_{\mathbf{q}j} = 2\pi\omega_{\mathbf{q}j} \sum_{\mathbf{k}nm} |g^{\mathbf{q}j}_{(\mathbf{k}+\mathbf{q})m;\mathbf{k}n}|^2 \delta(\varepsilon_{\mathbf{k}n} - \varepsilon_F)\delta(\varepsilon_{(\mathbf{k}+\mathbf{q})m} - \varepsilon_F), \tag{12}$$

where $\varepsilon_{(\mathbf{k}+\mathbf{q})m}$ and $g^{\mathbf{q}j}_{(\mathbf{k}+\mathbf{q})m;\mathbf{k}n}$ denote the energies of bands and the electron-phonon matrix element, respectively. The additive contribution from each vibrational mode to the electron-phonon coupling parameter is determined from the following equation:

$$\lambda_{\mathbf{q}j} = \frac{\gamma_{\mathbf{q}j}}{\pi\hbar N(\varepsilon_F)\omega^2_{\mathbf{q}j}}. \tag{13}$$

The average electron-phonon coupling λ is the summation of $\lambda_{\boldsymbol{q}j}$ over all phonon modes ($\boldsymbol{q}$j) in the IBZ,

$$\lambda = \sum_{\boldsymbol{q}j} \lambda_{\boldsymbol{q}j} W(\boldsymbol{q}). \tag{14}$$

Here, $W(\boldsymbol{q})$ is the weight of a sampling $\boldsymbol{q}$ point in the IBZ. The value of logarithmically averaged frequency $\omega_{\ln}$ can be derived from the following equation [47–51]:

$$\omega_{\ln} = exp\left(\frac{1}{\lambda}\sum_{\boldsymbol{q}j} \lambda_{\boldsymbol{q}j} \ln\omega_{\boldsymbol{q}j}\right). \tag{15}$$

Then, T_c is evaluated from the Allen-Dynes modified McMillan equation [51] which is given as

$$T_c = \frac{\omega_{\ln}}{1.2} \exp\left(-\frac{1.04(1+\lambda)}{\lambda - \mu^*(1 + 0.62\lambda)}\right). \tag{16}$$

Here, where μ^* is a Coulomb pseudopotential and its value changes between 0.10 and 0.16 [51]. In our calculations, we have decided to use the average of these limiting values, i.e., $\mu = 0.13$. The electronic specific heat coefficient γ for all the studied compounds can be derived from the calculated values of $N(E_F)$ and λ using the formula

$$\gamma = \frac{1}{3}\pi^2 k_B^2 N(E_F)(1 + \lambda). \tag{17}$$

We have to mention that all the above summations have been carried out by using a $4 \times 4 \times 4$ $\boldsymbol{q}$-point mesh, which do not contain any unstable phonon modes. Finally, we mention that the numerical values of $\alpha^2F(\omega)$, λ, $\omega_{\ln}$ and T_c have obtained using the executable "lambda.x," which is a part of QEP [46–48].

III. RESULTS

A. Structural, elastic, and mechanical properties

All the studied LaX_3 compounds possess the $AuCu_3$-type simple cubic crystal structure belonging to the space group $Pm\bar{3}m$. The structure of these compounds, shown in Fig. 1, contains one molecule with four atoms per unit cell, with one La atom located at 1a (0, 0, 0) and three X atoms at 2b (1/2, 1/2, 0). Thus the structural information is completely identified by the lattice parameter a. The calculated values for the equilibrium lattice parameter (a), the bulk modulus (B), and its pressure derivative (B') with and without SOC are presented in Table I along with existing experimental [30,31,43] and theoretical [41,42] results. The calculated lattice constants for LaX_3 compare very well with previous experimental [30,31,43] and theoretical values [41,42]. In particular, the calculated lattice parameters for these intermetallic compounds with and without SOC are found to differ by less than 2% from their experimental

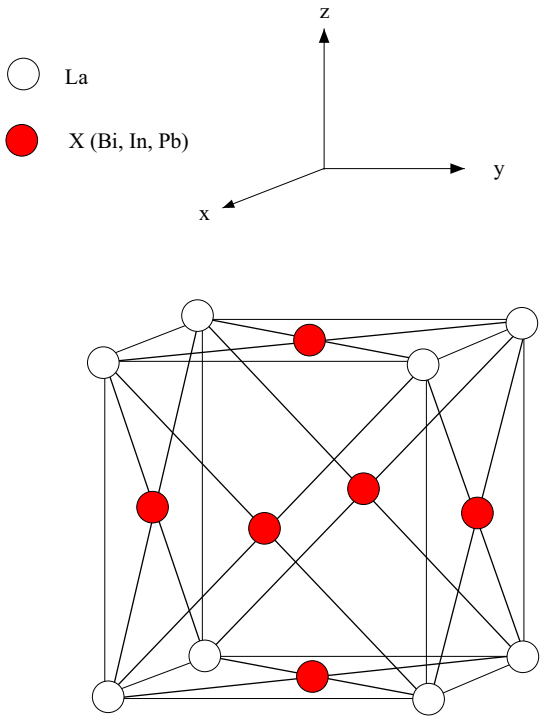

FIG. 1. The $AuCu_3$-type crystal structure of $LaIn_3$, $LaPb_3$, and $LaBi_3$.

values [30,31,43]. The presented values of bulk modulus for $LaIn_3$ and $LaPb_3$ materials are in gratifying agreement with previous LDA results [41], with a maximum difference of 5.0% for $LaPb_3$. However, our LDA results for the bulk modulus of $LaIn_3$ and $LaPb_3$ considerably differ from their corresponding GGA values [42], with a maximum difference of 28% for $LaIn_3$. This difference can be associated with the different exchange-correlation approximations used by our work and the work of Abraham *et al.* [42]. It is well established that GGA functionals produce larger equilibrium lattice constant than the LDA functional. This explains much of the differences between the LDA and GGA tabulated in Tabes I, II, III, and V. We would thus expect reduction in values of $N(E_F)$ and softening in phonon frequencies when GGA functionals are used.

As can be seen from Table I, the influence of SOC on the structural properties (a, B, and B') increases with increasing the mass of X atom. For example, the values of a, B, and B' for $LaPb_3$ ($LaBi_3$) change by 0.08% (0.14%), 2.64% (3.64%), and 5.50% (8.33%), respectively, with inclusion of the SOC. The calculated values of the three independent elastic constants for LaX_3 are presented in Table I along those reported in previous theoretical calculations [41,42]. However, no experimental results are available for comparison. Comparison of our results with previous LDA results [41] for $LaIn_3$ and $LaPb_3$ exhibits an acceptable agreement with a maximum difference of 14% for the C_{44} value of $LaPb_3$. However, our LDA results and previous GGA [42] results differ from each other by up to 33% due to the different exchange-correlation approximations used by these theoretical works. The elastic constants of $LaIn_3$ are affected by the SOC up to 1.3% due to the lighter mass of In atom as compared to the masses of Pb and Bi atoms. However, the maximum difference for $LaPb_3$ and $LaBi_3$ is around 5% for C_{11} and 21% for C_{44}, respectively. The calculated elastic constants lead us to examine the mechanical stability of crystal systems. In order to be mechanically stable, the cubic systems have to meet the well-known Born's stability criteria [67]: $C_{11} > C_{12}$, $C_{44} > 0$, and $C_{11} + 2C_{12} > 0$. The calculated value of these three independent elastic constants for all the studied compounds, presented in Table I, obey the Born's stability criteria [67], suggesting that these compounds are mechanically stable in their $AuCu_3$ type structure. Various other crucial elastic parameters are the Young's modulus E, shear modulus G_H, anisotropic factor A, Poisson's ratio σ, B/G_H, and Cauchy's pressure ($C_p = C_{12} - C_{44}$) for LaX_3, which are also derived from the second-order elastic constants, are presented in Table II along with previous theoretical results [41,42]. The calculated values of these elastic parameters for $LaIn_3$ and $LaPb_3$ are comparable with their counterpatterns in previous LDA calculations [41]. However, their calculated values considerably differ from their GGA counterpatterns [42], which we again believe arise from the differences in the values of second-order elastic constants between our calculations and

TABLE I. Lattice parameter a, bulk modulus B, its pressure derivative B', and second-order elastic constants (C_{11}, C_{12}, and C_{44}) for $LaIn_3$, $LaPb_3$, and $LaBi_3$ and their comparison with previous experimental and theoretical results.

Source	a(Å)	B(GPa)	B′	C_{11} (GPa)	C_{12} (GPa)	C_{44} (GPa)
$LaIn_3$ with SOC	4.656	64.5	4.63	108.81	42.19	34.50
$LaIn_3$ without SOC	4.658	64.3	4.59	109.19	41.85	34.97
Experimental [31]	4.739					
FP-LAPW method within LDA [41]	4.660	64.0		103.9	44.5	37.7
FP-LAPW method within GGA [42]	4.743	50.4	4.63	81.85	32.91	29.93
$LaPb_3$ with SOC	4.832	58.9	4.79	79.89	48.49	30.46
$LaPb_3$ without SOC	4.836	60.5	4.54	75.89	52.80	30.55
Experimental [30]	4.903					
Experimental [31]	4.905					
FP-LAPW method within LDA [41]	4.838	62.0		83.5	50.5	35.8
FP-LAPW method within GGA [42]	4.920	49.0	5.09	74.90	42.48	20.54
$LaBi_3$ with SOC	4.916	60.9	4.55	67.36	57.67	24.56
$LaBi_3$ without SOC	4.909	63.2	4.20	77.44	56.08	30.94
Experimental [43]	4.990					

TABLE II. Calculated values of Young's modulus E, shear modulus G_H, anisotropic factor A, Poisson's ratio σ, B/G_H, and Cauchy's pressure ($C_p = C_{12} - C_{44}$) for LaX_3 (X = In, Pb, and Bi) and their comparison with theoretical results.

Source	E (GPa)	G_H(GPa)	A	σ	B/G_H	C_p (GPa)
$LaIn_3$ with SOC	86.77	34.02	1.04	0.28	1.90	7.69
$LaIn_3$ without SOC	87.68	34.45	1.04	0.27	1.87	6.88
FP-LAPW method within LDA [41]	87.30	34.30	1.27	0.27	1.89	6.80
FP-LAPW method within GGA [42]	69.79	27.61	1.22	0.26	1.78	2.98
$LaPb_3$ with SOC	61.88	23.35	1.94	0.33	2.52	18.03
$LaPb_3$ without SOC	55.71	20.69	2.65	0.35	2.92	22.25
FP-LAPW method within LDA [41]	68.90	26.20	2.17	0.31	2.33	14.70
FP-LAPW method within GGA [42]	50.19	18.68	1.27	0.34	2.85	21.94
$LaBi_3$ with SOC	36.44	13.01	5.06	0.40	4.68	31.11
$LaBi_3$ without SOC	54.80	20.21	2.89	0.36	3.13	25.14

previous GGA calculations [42]. The effect of SOC on the values of E, G_H, A, σ, B/G_H, and C_p for $LaIn_3$ is not too large but this effect is considerably larger for the two remaining superconductors. For example, the values of A for $LaPb_3$ and $LaBi_3$ change within 27% and 43%, respectively. The Young's modulus can be used to provide a measure of the stiffness of the material: the larger the value of Young's modulus, the stiffer will be the material. In our calculations, the largest value of Young's modulus is calculated for $LaIn_3$, which means that it is the hardest compound among all the studied compounds. To the best of our knowledge, there are mainly three ways [68–70] to decide the brittleness and ductility of the material: the ratio of bulk to shear modulus B/G_H, Possion's ratio σ, and Cauchy's pressure C_p. In general, the value of $B/G_H > 1.75$, the value of $\sigma > 0.26$, and the value of C_P being positive signal that the material behaves in ductile manner, and vice versa. As presented in Table II, the values of B/G_H and σ are larger than 1.75 and 0.26, respectively, while the value of C_p is always positive. Thus all the considered materials behave in ductile manner. Furthermore, we have to mention that the largest values of B/G_H, σ, and C_p and the smallest values of E and G_H that have been observed for $LaBi_3$. Thus we can conclude that $LaBi_3$ is expected to be softer and more easily machinable compared to two remaining superconductors.

The calculated values of sound velocities (V_T, V_L, and V_M) and Debye temperature (Θ_D) for LaX_3 are presented in Table III, together with available experimental [32,37] and theoretical results [41,42]. Once again, the effect of SOC on the values of V_T, V_L, V_M, and Θ_D for $LaIn_3$ is negligible while these values for $LaPb_3$ and $LaBi_3$ are considerably changed with the inclusion SOC. Our results with SOC for $LaIn_3$ and $LaPb_3$ compare very well with previous LDA results for them [41]. However, the calculated values of V_T, V_L, V_M, and Θ_D with SOC for these superconductors are significantly different from their GGA counterpatterns [42]. This difference can be linked to differences in the values of B, C_{11}, C_{12}, C_{44}, E, and G_H between our LDA results and previous GGA results [42]. As displayed in Table III, the values of V_T, V_L, V_M, and Θ_D increase with decreasing mass of X atom. Finally, the calculated values of Debye temperatures for $LaIn_3$ and $LaPb_3$ with SOC (without SOC) are found to be 234 K (235 K) and 158 K (149 K), respectively, which are comparable with their experimental values 194 and 147 K [32,37].

B. Electronic properties

The calculated electronic structures of $LaIn_3$, $LaPb_3$, and $LaBi_3$ with and without SOC are displayed in Fig. 2. In general agreement with previous works [41,43], the electronic

TABLE III. Calculated transverse (V_T), longitudinal (V_L), average elastic wave velocities (V_M), and Debye temperature (Θ_D) of $LaBi_3$, $LaPb_3$, and $LaIn_3$ superconductors and their comparison with previous experimental and theoretical results.

Source	V_T (m/s)	V_L (m/s)	V_M(m/s)	Θ_D (K)
$LaBi_3$ with SOC	1103	2704	1248	120
$LaBi_3$ without SOC	1371	2896	1543	149
$LaPb_3$ with SOC	1444	2877	1619	158
$LaPb_3$ without SOC	1362	2810	1530	149
Experimental [37]				147
FP-LAPW method within LDA [41]	1530	2940	1712	168
FP-LAPW method within GGA [42]	1603	3273	1799	95
$LaIn_3$ with SOC	2069	3716	2304	234
$LaIn_3$ without SOC	2083	3726	2319	235
Experimental [32]				194
Experimental [37]				170
FP-LAPW method within LDA [41]	2080	3720	2315	235
FP-LAPW method within GGA [42]	2316	4082	2573	140

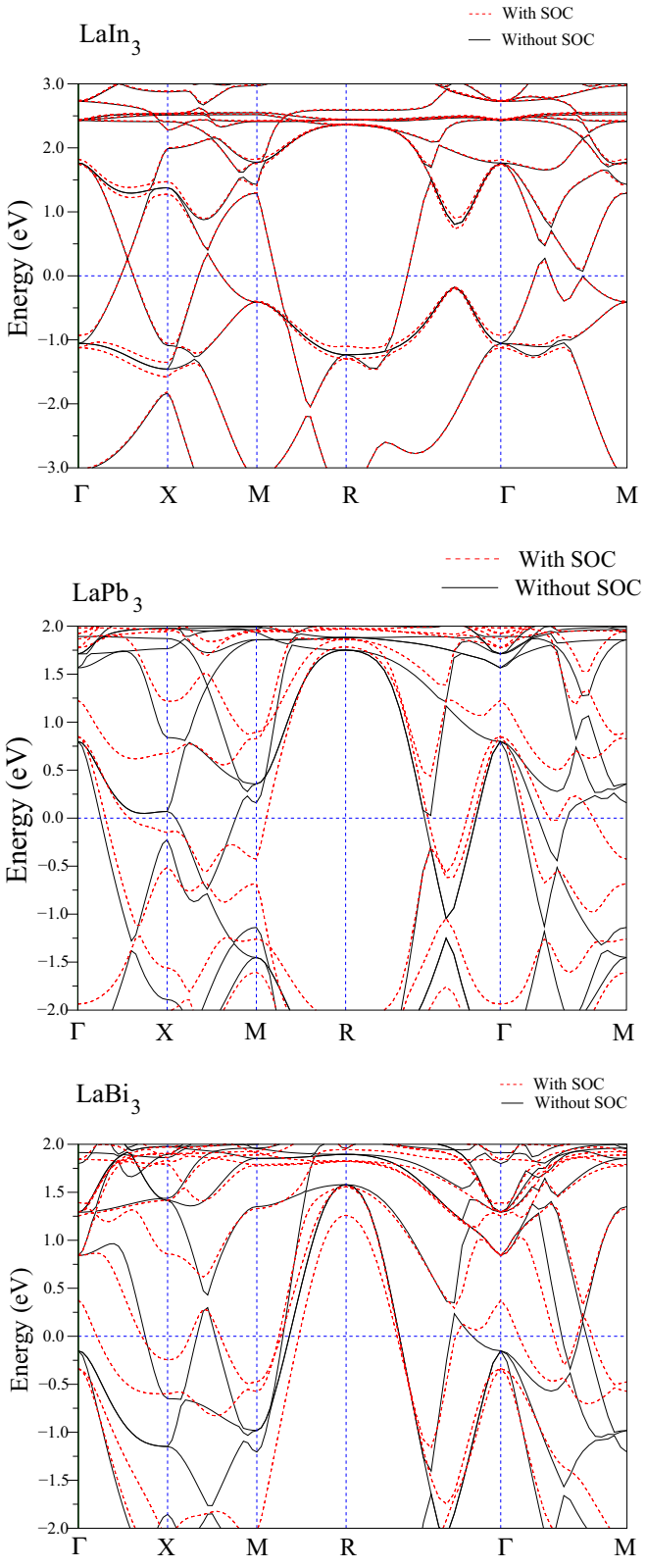

FIG. 2. Electronic band structures of $LaIn_3$, $LaPb_3$, and $LaBi_3$ for high-symmetry lines of the simple cubic lattice with and without spin-orbit coupling (SOC). The Fermi level is chosen to be 0 eV.

structures of these superconductors reveal metallic character since at least one band crosses the Fermi level along all the considered symmetry directions. The inclusion of SOC causes some bands to split at the high-symmetry points in the Brillouin zone. At the zone center, the effect of SOC is more obvious for all the considered superconductors. In particular, the largest splitting at the Γ point is found to be 0.2 eV for $LaIn_3$, 0.4 eV for $LaPb_3$, and 0.7 eV for $LaBi_3$. These band splittings are consistent with the effect of SOC increasing with the mass of X atom since the strength of SOC depends on Z^4 (Z is the atomic number).

In order to investigate the nature of electronic bands, the total and partial density of states (DOS) with and without SOC of $LaIn_3$ are illustrated in Fig. 3(a). It is found that the effect of SOC on the total DOS of $LaIn_3$ is very small. A critical assessment of partial DOS indicates that the DOS features in the low part of occupied bands (typically 3.0 eV below the Fermi level) mainly consist of hybridized In 5s, In 5p, La 6s, and La 5d orbitals with a dominant contribution from the first one. The majority of In 5p states exists between −3.0 and 1.0 eV and makes a considerable hybridization with the 5d states of La. The value of the DOS at the Fermi level [$N(E_F)$] is found to be 2.191 states/eV, which is almost equal to its experimental value of 2.190 states/eV derived from the heat-capacity measurement [33,34]. La and In electronic states contribute to the value of $N(E_F)$ up to 35% and 65%, respectively. The contributions of La 5d and In 5p states to $N(E_F)$ are approximately 33% and 48%, respectively. When SOC is not considered, the value of $N(E_F)$ for $LaIn_3$ decreases by around less than 2%, from 2.191 to 2.154 states/eV. This small decrease suggests that the influence of SOC on the electronic bands of $LaIn_3$ close to the Fermi level is small.

The total and partial DOS with and without SOC for $LaPb_3$ are presented in Fig. 3(b). This comparison shows that the influence of SOC on the total DOS of $LaPb_3$ is more significant than for $LaIn_3$. This is due to the heavier mass of Pb than that of In. The valence DOS of $LaPb_3$ splits into two parts. The lower part extending from −11.2 to −6.2 eV consists almost entirely of Pb 6s states with much smaller contributions from La 6p, Pb 6p, and La 5d states. This part is separated from the near-Fermi bands (the second part from −4.5 eV to the Fermi level) by a gap of 1.7 eV. The second region is mainly contributed by Pb 6p states with a significant contribution from La 5d states. Thus, in this region close to the Fermi level, a significant hybridization between Pb 6p and La 5d states exists. The DOS at the Fermi level, $N(E_F)$, is 2.962 states/eV, which lies between its GGA value [42] of 2.40 states/eV and its previous LDA value [41] of 3.41 states/eV. The value of $N(E_F)$ for $LaPb_3$ is considerably higher than that for $LaIn_3$. La and Pb electronic states contribute to the value of $N(E_F)$ up to approximately 25% and 75%, respectively. In particular, the orbital contributions at the Fermi level consist of La 5d (23%) and Pb 6p (65%). If we ignore SOC, the value of $N(E_F)$ decreases by around 19%, from 2.962 to 2.499 states/eV. It is worthy to mention that the origin of this large decrease originates mainly from the decrease from 1.925 to 1.5244 states/eV in the contribution from Pb 6p states when SOC is ignored. As a consequence, we can conclude that the effect of SOC on the energy band close to the Fermi level is much more profound for $LaPb_3$ rather than $LaIn_3$ due to the heavier mass of Pb than the mass of In.

Figure 3(c) displays the total and partial DOS with and without SOC for $LaBi_3$. At first glance, the total and partial

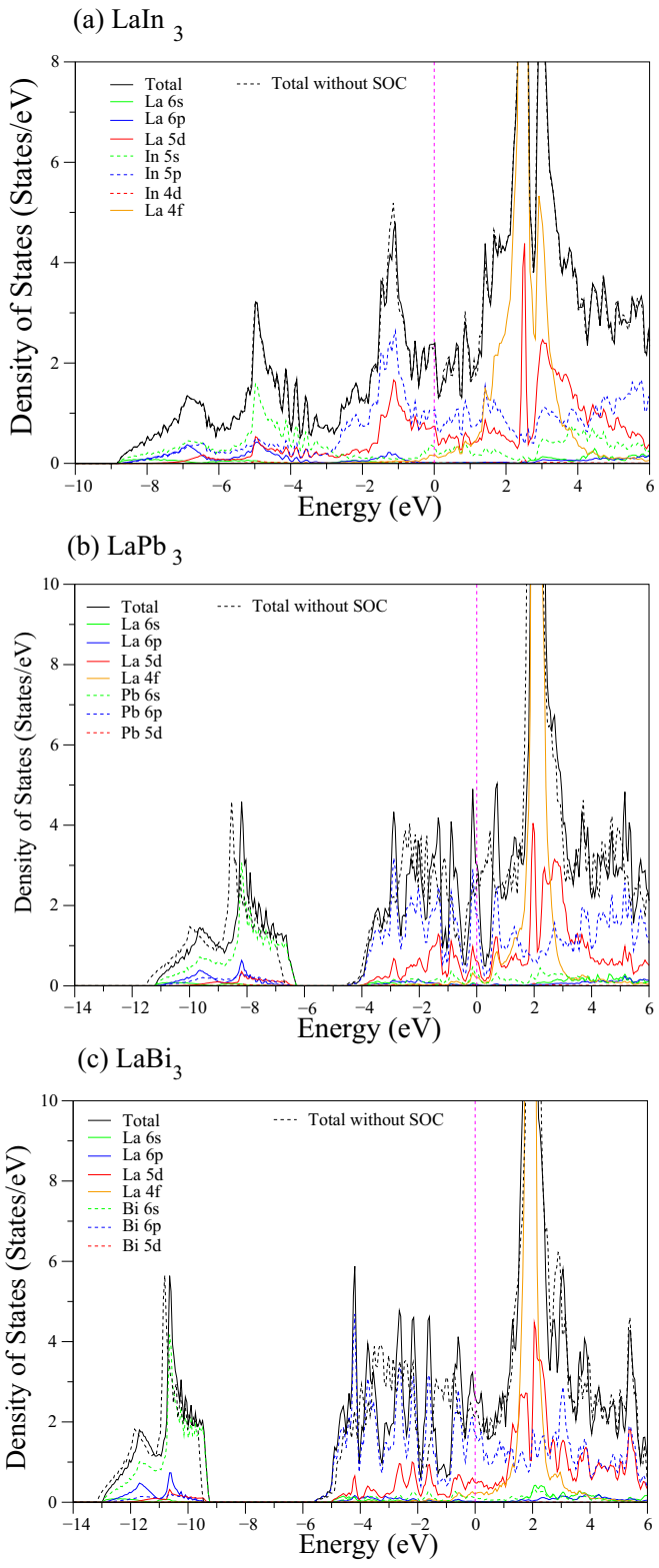

FIG. 3. Total and partial density of states with SOC for (a) $LaIn_3$, (b) $LaPb_3$, and (c) $LaBi_3$. Total density of states without SOC for all the considered compounds are also shown by a black dashed curve. The Fermi level is chosen to be 0 eV.

DOS of $LaBi_3$ look similar to those of $LaPb_3$. Similar to $LaPb_3$, the partial valence DOS of $LaBi_3$ can be divided into two obvious regions. The lower region extending from −13.0 to −9.2 eV stems almost entirely from Bi 6*s* states with much smaller contributions from La 6*p*, Bi 6*p*, and La 5*d* states. The remaining region until the Fermi level shows a dominance of Bi 6*p* states with much less contributions from La 5*d* states. In the present work, the value of $N(E_F)$ for $LaBi_3$ is found to be 2.685 states/eV, which is larger than that for $LaIn_3$ but smaller than that for $LaPb_3$. The value of $N(E_F)$ decreases by around 30%, from 2.685 to 2.063 states/eV, when SOC is ignored. This decrease is larger than the corresponding decrease for the other two La compounds studied here. Thus it is expected that the effect of SOC on the electron-phonon interaction in $LaBi_3$ will be larger than that in the other two compounds. A critical examination of the partial DOS for $LaBi_3$ shows that $N(E_F)$ is contributed approximately by 22% from La electronic states and 78% Bi electronic states. In particular, La *d* and Bi *p* states alone contribute up to 20% and 73%.

TABLE IV. Calculated zone-center phonon frequencies (ν in THz) and their eigencharacters λ for $LaIn_3$, $LaPb_3$, and $LaBi_3$. IR and S denote infrared active and silent vibrations, respectively.

Mode	T_{1u}	T_{2u}	T_{1u}
$LaIn_3$ (ν with SOC)	2.27	2.87	4.49
$LaIn_3$ (ν without SOC)	2.25	2.86	4.48
Eigencharacters	La+In	In	La+In
Active	IR	S	I
$LaPb_3$ (ν with SOC)	1.55	2.17	3.58
$LaPb_3$ (ν without SOC)	1.78	2.22	3.67
Eigencharacters $LaPb_3$	La+Pb	Pb	La+Pb
Active	IR	S	I
$LaBi_3$ (ν with SOC)	2.23	2.08	3.07
$LaBi_3$ (ν without SOC)	2.22	2.20	3.14
Eigencharacters	La+Bi	Bi	La+Bi
Active	IR	S	I

C. Effect of SOC on phonons

The zone-center phonon modes of LaX_3 can be grouped by the irreducible representation of the point group O_h ($m\bar{3}m$). As derived from the point group theory, the symmetries of the zone-center optical vibrations can be stated as

$$\Gamma(O_h) = 2T_{1u} + T_{2u},$$

where the T_{1u} vibrations are infrared (IR) active, and T_{2u} is optically silent. For all the studied compounds, the calculated frequencies of these zone-center optical vibrations with and without SOC are presented in Table IV. The T_{2u} mode is totally characterized by the vibrations of *X* atoms while the T_{1u} modes arise from the hybridized vibrations of La and *X* atoms. Table IV reveals that the influence of SOC on the zone-center vibrations of $LaIn_3$ is negligible while this effect is more pronounced for the other two superconductors. In particular, upon inclusion of SOC, the lower frequency T_{1u} vibration of $LaPb_3$ becomes softer by around 13%, while the T_{2u} vibration of $LaBi_3$ gets softer by around 5%. However, it is worth to mention that this softening is less than 1% for the zone-center vibrations of $LaIn_3$ because of the smaller mass of In as compared to the masses of Pb and Bi atoms.

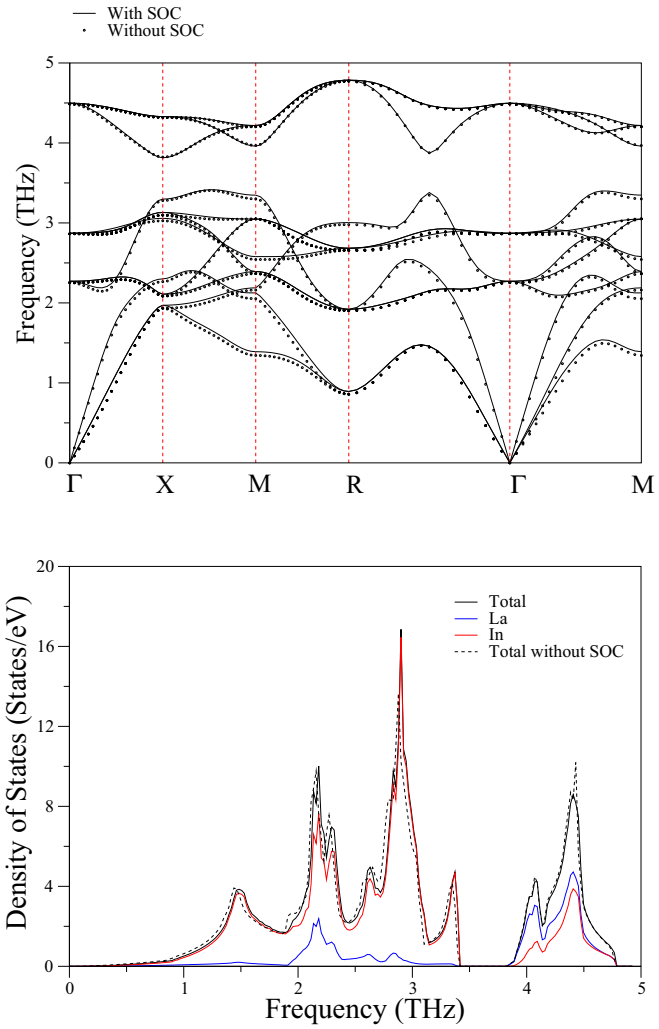

FIG. 4. Phonon dispersion curves and phonon density of states with SOC for $LaIn_3$. Phonon spectrum without SOC is shown by open circles while the total phonon density of states without SOC is shown by the dashed line.

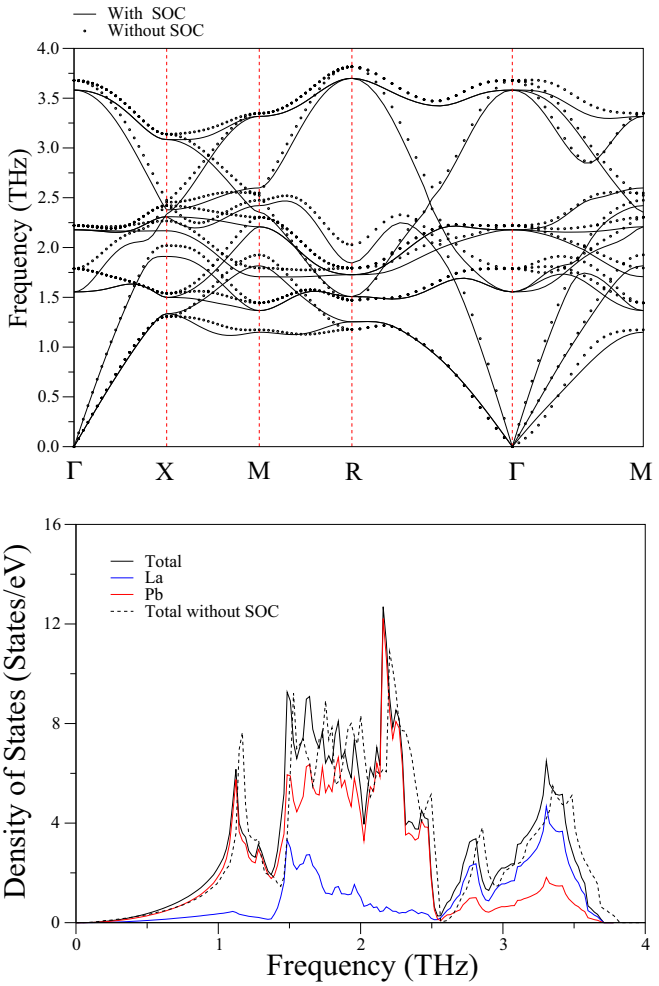

FIG. 5. Phonon dispersion curves and phonon density of states with SOC for $LaPb_3$. The phonon spectrum without SOC is shown by open circles while the total phonon density of states without SOC is shown by the dashed line.

Accurate determination of the electron-phonon coupling parameter requires the knowledge of full phonon dispersion curves and phonon density of states. These features for $LaIn_3$ are displayed in Fig. 4. The phonon spectrum can be divided into two apparent parts: one broad part extending up to 3.4 THz, and one narrower part in the frequency ranges of 3.8 to 4.8 THz. All phonon branches in these two regions exhibit significant dispersion. It can be clearly noticed that the phonon dispersion curves with and without SOC almost coincide between each other, except that with the inclusion of SOC the acoustic and lower optical modes become a little harder. The partial DOS exhibits a dominance of In atoms in the broad region, in spite of La atom having a heavier mass than In atoms. This reveals that the three acoustic phonon branches of $LaIn_3$ stem mainly from the vibrations of In atoms. On the other hand, strong La-In hybridization exists in the narrower region.

The calculated phonon dispersion curves and phonon density of states for $LaPb_3$ are depicted in Fig. 5. In contrast to $LaIn_3$, there is no gap in their phonon dispersion curves and phonon density of states. The La-related and X-related phonon DOS cover the whole range of phonon frequencies, leaving no gap in their phonon DOS. In particular, the heavier X atoms dominate the low-frequency region below 2.6 THz, while a dominance of lighter La atom exist above this frequency. With the inclusion of SOC, all phonon modes, except for long-wavelength acoustic modes, become much softer. The long-wavelength transverse acoustic modes, however, have become harder along Γ-M and in the neighbourhood of the R point. As a result, the peaks in the phonon density of states have shifted to lower frequencies.

The calculated phonon dispersion curves and phonon density of states for $LaBi_3$ are depicted in Fig. 6. Similar to $LaPb_3$, the phonon modes in $LaBi_3$ have become softer upon the inclusion of SOC, and the peaks in the phonon density of states have shifted to lower frequencies. Our calculations have revealed imaginary frequencies for the lower branch long-wavelength transverse modes when SOC is not included, indicating that the SOC is important in ensuring a dynamically stable structure for $LaBi_3$.

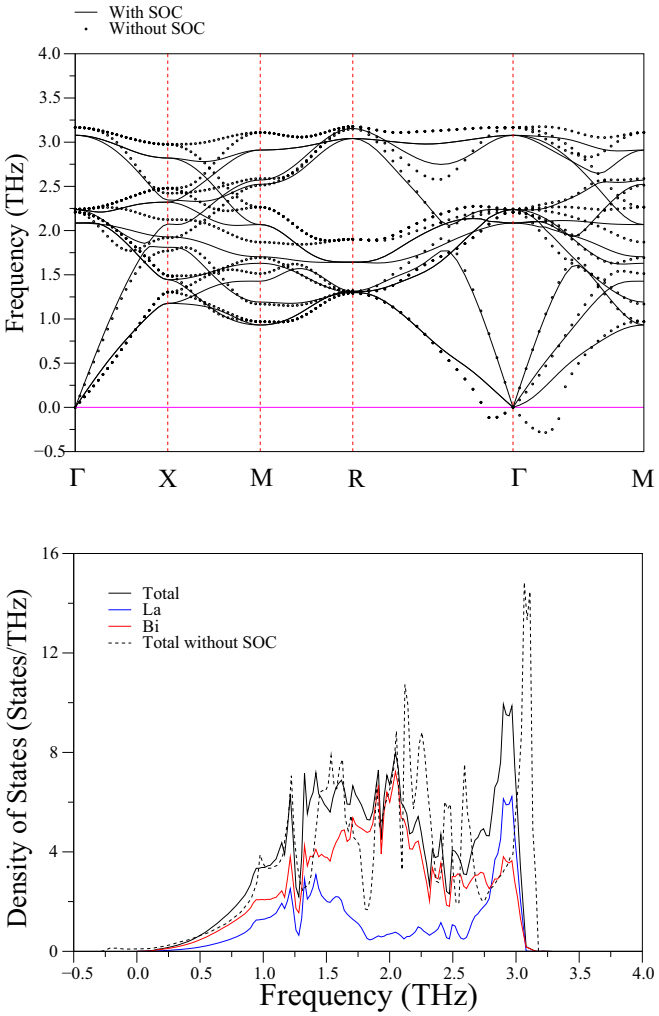

FIG. 6. Phonon dispersion curves and phonon density of states with SOC for $LaBi_3$. Phonon spectrum without SOC is shown by open circles while the total phonon density of states without SOC is shown by the dashed line.

D. Electron-phonon interaction

The electron-phonon interaction in BCS superconductors is discussed in terms of the electron-phonon coupling parameter λ. According to the McMillan-Hopfield expression, this is given as

$$\lambda = \frac{N(E_F) < I^2 >}{M < \omega^2 >}, \tag{18}$$

where $< I^2 >$, M, and $< \omega^2 >$ are the Fermi surface average of squared electron-phonon coupling interaction, the mass involved, and the average of squared phonon frequencies. Clearly, for a material of mass M, larger λ values require larger $N(E_F)$ and smaller $< \omega^2 >$. Our calculations suggest that both in $LaPb_3$ and $LaBi_3$ the value of λ has opposite contributions from $N(E_F)$ and $< \omega^2 >$. From the results presented above (Figs. 4 and 5), we note the large decrease in the value of $N(E_F)$ without SOC will generate a smaller value for λ. However, the softening of phonon modes with the inclusion of SOC possesses a potential to produce a larger value of λ.

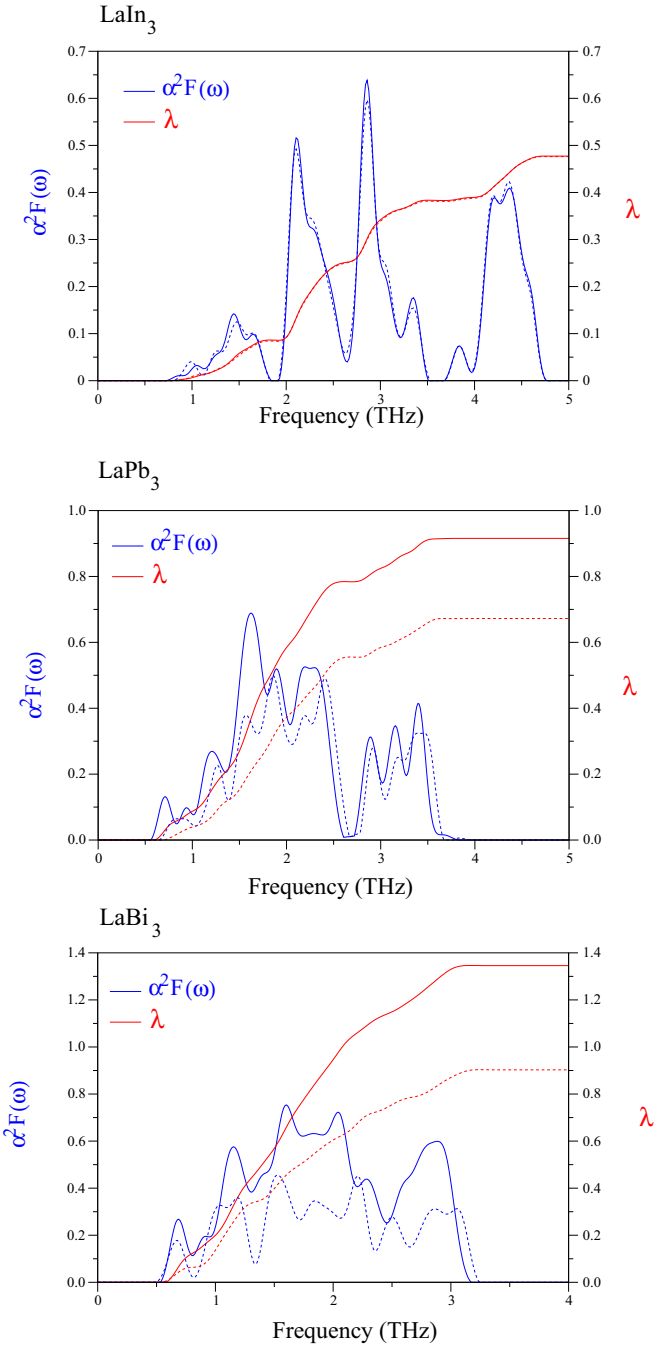

FIG. 7. Eliashberg spectral function $\alpha^2 F(\omega)$ (blue line) and integrated electron-phonon coupling parameter λ (red line) for $LaIn_3$, $LaPb_3$, and $LaBi_3$. Our results without SOC are presented by dashed lines.

Figure 7 presents the Eliashberg spectral function $\alpha^2 F(\omega)$ and the frequency variation of the average electron-phonon coupling parameter λ for all the considered compounds. For comparison, our results for $\alpha^2 F(\omega)$ and λ without SOC are also included in this figure. For $LaIn_3$, $\alpha^2 F(\omega)$ and λ with SOC almost coincide with their counterpatterns without SOC. This result is largely expected since the existence of SOC makes a negligible influence on its electronic and phonon properties. The Eliashberg spectral function for $LaIn_3$ emphasizes that its phonon branches below the gap region make the dominant

TABLE V. The calculated values of the physical quantities related to superconductivity in LaX_3 (X = In, Pb, and Bi) with SOC (without SOC).

Superconductor	$N(E_F)$ (states/eV)	ω_{ln} (K)	λ	$\gamma(\frac{\text{mJ}}{\text{mol K}^2})$	T_c (K)
$LaIn_3$	2.191 (2.154)	120.62 (120.89)	0.477 (0.476)	7.61 (7.47)	0.694 (0.687)
Experimental [31]					0.70
Experimental [32]			0.59	6.28	
Experimental [33,34]	2.19		0.44		
Experimental [38]					0.70
ASW [39]	1.70		0.10		
LMTO [40]	1.89				
FP-LAPW method within LDA [41]	2.58				
FP-LAPW method within GGA [42]	1.96				
$LaPb_3$	2.962 (2.499)	83.41 (91.43)	0.916 (0.672)	13.33 (9.82)	4.232 (2.161)
Experimental [30]					4.05
Experimental [31]					4.10
Experimental [35]					4.18
FP-LAPW method within LDA [41]	3.41				
FP-LAPW method within GGA [42]	2.40				
$LaBi_3$	2.685 (2.063)	74.71 (75.27)	1.346 (0.903)	14.80 (9.225)	6.876 (3.710)
Experimental [43]					7.30

contribution to its λ value. These phonon branches contribute about 80% (0.3816) to the total value of λ, but the phonon bands above the gap region make a contribution of about 20% (0.0954) to the total value of λ. The large contribution to λ from the low-frequency phonon branches is totally expected since these phonon modes are mainly localized on the In atoms which dominate the electronic bands close to the Fermi level with their p electrons. The inclusion of SOC increases the strength of dominant peaks in the Eliashberg spectral functions of $LaPb_3$ and $LaBi_3$. Hence the SOC-caused enhancement of their λ values can be related to both a softening of their phonon dispersion curves and an increase in their electron-phonon coupling matrix elements. In particular, we find that the presence of SOC increases the value of λ by around 36% (from 0.672 to 0.916) for $LaPb_3$ and around 49% (from 0.903 to 1.346) for $LaBi_3$. A critical evaluation of the spectral function with SOC for both superconductors reveals that X-related vibrations below around 2.6 THz contribute about 85% for $LaPb_3$ and 88% for $LaBi_3$ to the value of λ due to the significant existence of Pb p (or Bi p) states close to the Fermi level.

The calculated values of the physical quantities with and without SOC related to superconductivity in all the studied compounds and their comparison with available experimental [30–35,38,43] and theoretical [39–42] results are presented in Table V. The calculated values of these quantities compare very well with their experimentally reported values [31–34,38]. Clearly, the values of $N(E_F)$, ω_{ln}, λ, γ, and T_c for $LaIn_3$ do not change considerably by the inclusion of SOC. The SOC considerably increases the λ values of $LaPb_3$ and $LaBi_3$, which gives rise to an increase in their T_c values. It is pleasing to note that the calculated T_c values of $LaPb_3$ and $LaBi_3$ are in good agreement with their experimental values of 4.18 and 7.30 K [35,43].

Now, we make a comparison of the superconducting parameters between these three superconductors. According to the McMillan-Hopfield expression and the Allen-Dynes modification of the McMillian formula, the superconducting transition temperature depends on three main factors, *viz.* the electronic DOS at the Fermi level $N(E_F)$, the logarithmic average phonon frequency ω_{ln}, and the strength of electron-phonon coupling parameter λ. The largest value of ω_{ln} for $LaIn_3$ confirms that phonon modes in this superconductor are much harder that those in two remaining superconductors. The harder phonon modes make its λ and T_c values much smaller than the corresponding values for $LaPb_3$ and $LaBi_3$. Although the $N(E_F)$ value of $LaPb_3$ is larger than that of $LaBi_3$, its T_c value is much lower than that of $LaBi_3$. This result strongly suggests that the difference between their T_c values can not be simply related to the difference in their $N(E_F)$ values, but requires analyzing their phonon properties. The smallest value of ω_{ln} for $LaBi_3$ reveals that phonon modes in $LaBi_3$ are much softer than those in $LaPb_3$. Thus the value of λ for $LaBi_3$ becomes considerably larger than that for $LaPb_3$, which makes the T_c value of the former higher than that of the later.

IV. SUMMARY

We have studied the role of spin-orbit coupling on the structural, elastic, mechanical, electronic, phonon, and electron-phonon interaction properties of LaX_3 (X = In, Pb, and Bi) using first-principles density functional calculations within the local density approximation. The inclusion of SOC makes more effect on the structural, elastic, and mechanical properties of $LaPb_3$ and $LaBi_3$ than those of $LaIn_3$ since the strength of this coupling depends on Z^4 (Z is the atomic number). The calculated values of the three independent elastic constants for all the studied compounds satisfy the well-known Born's stability criteria, pointing that they are all mechanically stable in their $AuCu_3$-type structure. The calculated values of polycrystalline elastic modulus for these superconductors reveal that $LaIn_3$ is the hardest compound among them. Furthermore, the results indicate that all the investigated compounds behave in ductile manner, but $LaBi_3$ is softer and more easily machinable than the two remaining compounds. The inclusion of SOC in the

electronic calculations causes splitting of some bands. This splitting is more apparent for $LaPb_3$ and $LaBi_3$ than $LaIn_3$ due to the heavier masses of Pb and Bi as compared to that of In. A critical assessment of our electronic results reveals that the bands near the Fermi level are mainly composed of X p orbitals, but the contribution of La $5d$ states can not be ignored.

The presence of SOC on the phonon properties of $LaIn_3$ is negligible, but this coupling makes some phonon modes softer for $LaPb_3$ and $LaBi_3$. Considering the calculated phonon dispersion curves of all the studied compounds, we observe that these superconductors are all dynamically stable in their $AuCu_3$. However, the noninclusion of SOC makes the lowest acoustic branch of $LaBi_3$ unstable along the R-Γ-M direction. The electron-phonon properties of $LaIn_3$ are almost unaffected by the inclusion of SOC. However, this coupling raises the strength of dominant peaks of the Eliashberg spectral functions of $LaPb_3$ and $LaBi_3$, which increases the value of λ from 0.672 to 0.903 for $LaPb_3$ and 0.916 to 1.346 for $LaBi_3$. Thus the SOC-caused enhancement of T_c in $LaPb_3$ and $LaBi_3$ can be associated with both a softening of their phonon dispersion curves and an increment in their electron-phonon coupling matrix elements. Finally, the superconducting transition temperature with SOC is determined to be 0.69 K for $LaIn_3$, 4.23 K for $LaPb_3$, and 6.87 K for $LaBi_3$, which agree very well with their experimental values of 0.70, 4.18, and 7.30 K. As a consequence, our results emphasize that the origin of superconductivity in $LaIn_3$, $LaPb_3$, and $LaBi_3$ can be explained very well by the electron-phonon interaction mechanism.

ACKNOWLEDGMENTS

Some of the calculations for this project were carried out using the computing facilities on the Intel Nehalem (i7) cluster (ceres) in the School of Physics, University of Exeter, United Kingdom.

[1] Y. Baer, H. R. Ott, J. C. Fuggle, and L. E. De Long, Phys. Rev. B **24**, 5384 (1981).
[2] K. Ikeda and K. A. Gschneidner, Phys. Rev. B **25**, 4623 (1982).
[3] H. Wehr, K. Knorr, F. N. Gygax, A. Schenck, and W. Studer, Phys. Rev. B **29**, 6381(R) (1984).
[4] C. L. Lin, J. Teter, J. E. Crow, T. Mihalisin, J. Brooks, A. I. Abou-Aly, and G. R. Stewart, Phys. Rev. Lett. **54**, 2541 (1985).
[5] C. Vettier, P. Morin, and J. Flouquet, Phys. Rev. Lett. **56**, 1980 (1986).
[6] Y.-Y. Chen, J. M. Lawrence, J. D. Thompson, and J. O. Willis, Phys. Rev. B **40**, 10766 (1989).
[7] U. Walter, E. Holland-Moritz, and Z. Fisk, Phys. Rev. B **43**, 320 (1991).
[8] Z. Kletowski, Solid State Commun. **81**, 297 (1992).
[9] A. P. Murani, Phys. Rev. B **28**, 2308(R) (1983).
[10] G. E. Grechnev, A. S. Panfilov, I. V. Svechkarev, K. H. J. Buschow, and A. Czopnik, J. Alloys Comp. **226**, 107 (1995).
[11] A. Hiess, J. X. Boucherle, F. Givord, and P. C. Canfield, J. Alloys Comp. **224**, 33 (1995).
[12] D. T. Adroja, B. D. Rainford, and A. G. M. Jansen, J. Magn. Magn. Mater. **140-144**, 1217 (1995).
[13] I. R. Walker, F. M. Grosche, D. M. Freye, and G. G. Lonzarich, Physica C **282-287**, 303 (1997).
[14] H. Suzuki, H. Kitazawa, T. Naka, J. Tang, and G. Kido, Solid State Commun. **107**, 447 (1998).
[15] D. Aoki, Y. Katayama, R. Settai, Y. Inada, Y. Onuki, H. Harima, and Z. Kletowski, J. Magn. Magn. Mater. **177-181**, 365 (1998).
[16] V. B. Pluzhnikov, A. Czopnik, O. Eriksson, G. E. Grechnev, and Yu. V. Fomenko, Low Temp. Phys. **25**, 670 (1999).
[17] V. B. Pluzhnikov, A. Czopnik, G. E. Grechnev, N. V. Savchenko, and W. Suski, Phys. Rev. B **59**, 7893 (1999).
[18] K. Kanai, Y. Tezuka, T. Terashima, Y. Muro, M. Ishikawa, T. Uozumi, A. Kotani, G. Schmerber, J. P. Kappler, J. C. Parlebas, and S. Shin, Phys. Rev. B **60**, 5244 (1999).
[19] R. Pietri and B. Andraka, Phys. Rev. B **62**, 8619 (2000)
[20] T. Ebihara, K. Koizumi, S. Uji, C. Terakura, T. Terashima, H. Suzuki, H. Kitazawa, and G. Kido, Phys. Rev. B **61**, 2513 (2000).
[21] Z. Kletowski, A. Czopnik, A. Tal, and F. der Boer, Physica B **281-282**, 163 (2000).
[22] M. Biasini, G. Kontrym-Sznajd, M. A. Monge, M. Gemmi, A. Czopnik, and A. Jura, Phys. Rev. Lett. **86**, 4616 (2001).
[23] S. Kawasaki, T. Mito, Y. Kawasaki, G.-q. Zheng, Y. Kitaoka, H. Shishido, S. Araki, R. Settai, and Y. Onuki, Phys. Rev. B **66**, 054521 (2002).
[24] M. Biasini, G. Ferro, and A. Czopnik, Phys. Rev. B **68**, 094513 (2003).
[25] L. P. Gor'kov and P. D. Grigoriev, Phys. Rev. B **73**, 060401(R) (2006).
[26] N. Harrison, S. E. Sebastian, C. H. Mielke, A. Paris, M. J. Gordon, C. A. Swenson, D. G. Rickel, M. D. Pacheco, P. F. Ruminer, J. B. Schillig, J. R. Sims, A. H. Lacerda, M.-T. Suzuki, H. Harima, and T. Ebihara, Phys. Rev. Lett. **99**, 056401 (2007).
[27] C. H. Wang, J. M. Lawrence, A. D. Christianson, E. A. Goremychkin, V. R. Fanelli, K. Gofryk, E. D. Bauer, F. Ronning, J. D. Thompson, N. R. de Souza, A. I. Kolesnikov, and K. C. Littrell, Phys. Rev. B **81**, 235132 (2010).
[28] N. Berry, E. M. Bittar, C. Capan, P. G. Pagliuso, and Z. Fisk, Phys. Rev. B **81**, 174413 (2010).
[29] R. D. Schmidt, E. D. Case, G. J. Lehr, and D. T. Morelli, Intermetallics **35**, 15 (2013).
[30] R. J. Gambino, N. R. Stemple, and A. M. Toxen, J. Phys. Chem. Solids **29**, 295 (1968).
[31] E. E. Havinga, H. Damsma, and M. H. van Maaren, J. Phys. Chem. Solids **31**, 2653 (1970).
[32] S. Nasu, A. M. Van Diepen, H. H. Neumann, and R. S. Craig, J. Phys. Chem. Solids **32**, 2773 (1971).
[33] A. M. Toxen, R. J. Gambino, and B. J. van der Hoeven, Physica **55**, 626 (1971).
[34] A. M. Toxen, R. J. Gambino, and L. B. Welsh, Phys. Rev. B **8**, 90 (1973).
[35] L. B. Welsh, C. L. Wiley, and F. Y. Fradin, Phys. Rev. B **11**, 4156 (1975).
[36] F. Canepa, G. A. Costa, and G. L. Olcese, Solid State Commun. **45**, 725 (1983).

[37] Z. Kletowski, R. Fabrowski, P. Slawinski, and Z. Henkie, J. Magn. Magn. Mater. **166**, 361 (1997).
[38] E M Bittar, C. Adriano, C. Giles, C. Rettori, Z. Fisk, and P. G. Pagliuso, J. Phys.: Condens. Matter **23**, 455701 (2011).
[39] D. Hackenbracht and J. Kubler, Z. Phys. B **35**, 27 (1979).
[40] Tang Shao-ping, Zhang Kai-ming, and Xie Xi-de, J. Phys.: Condens. Matter **1**, 2677 (1989).
[41] S. Ram, V. Kanchana, A. Svane, S. B. Dugdale, and N. E. Christensen, J. Phys.: Condens. Matter **25**, 155501 (2013).
[42] J. A. Abraham, G. Pagare, S. S. Chouhan, and S. P. Sanyal, Comput. Mater. Sci. **81**, 423 (2014).
[43] T. Kinjo, S. Kajino, T. Nishio, K. Kawashima, Y. Yanagi, I. Hase, T. Yanagisawa, S. Ishida, H. Kito, and N. Akeshita, Supercond. Sci. Technol. **29**, 03LT02 (2016).
[44] W. L. McMillian, Phys. Rev. **167**, 331 (1975).
[45] R. Heid, K.-P. Bohnen, I. Yu. Sklyadneva, and E. V. Chulkov, Phys. Rev. B **81**, 174527 (2010).
[46] http://www.quantum-espresso.org/.
[47] P. Giannozzi, S. Baroni, N. Bonini, M. Calandra, R. Car, C. Cavazzoni, D. Ceresoli, G. L. Chiarotti, M. Cococcioni, I. Dabo, A. D. Corso, S. de Gironcoli, S. Fabris, G. Fratesi, R. Gebauer, U. Gerstmann, C. Gougoussis, A. Kokalj, M. Lazzeri, L. Martin-Samos, N. Marzari, F. Mauri, R. Mazzarello, S. Paolini, A. Pasquarello, L. Paulatto, C. Sbraccia, S. Scandolo, G. Sclauzero, A. P. Seitsonen, A. Smogunov, P. Umari, and R. M. Wentzcovitch, J. Phys.: Condens. Matter **21**, 395502 (2009).
[48] P. Giannozzi, O. Andreussi, T. Brumme, O. Bunau, M. Buongiorno Nardelli, M. Calandra, R. Car, C. Cavazzoni, D. Ceresoli, M. Cococcioni, N. Colonna, I. Carnimeo, A. Dal Corso, S. de Gironcoli, P. Delugas, R. A. DiStasio Jr., A. Ferretti, A. Floris, G. Fratesi, G. Fugallo, R. Gebauer, U. Gerstmann, F. Giustino, T. Gorni, J. Jia, M. Kawamura, H.-Y. Ko, A. Kokalj, E. Küçükbenli, M. Lazzeri, M. Marsili, N. Marzari, F. Mauri, N. L. Nguyen, H.-V. Nguyen, A. Otero-de-la-Roza, L. Paulatto, S. Poncé, D. Rocca, R. Sabatini, B. Santra, M. Schlipf, A. P. Seitsonen, A. Smogunov, I. Timrov, T. Thonhauser, P. Umari, N. Vast, X. Wu, and S. Baroni, J. Phys.: Condens. Matter **29**, 465901 (2017).
[49] A. B. Migdal, Zh. Eksp. Teor. Fiz. **34**, 1438 (1958) [Sov. Phys. JETP **7**, 996 (1958)].
[50] G. M. Eliashberg, Zh. Eksp. Teor. Fiz. **38**, 966 (1960) [Sov. Phys. JETP. **11**, 696 (1960)].
[51] P. B. Allen and R. C. Dynes, Phys. Rev. B **12**, 905 (1975).
[52] D. M. Ceperley and B. I. Alder, Phys. Rev. Lett. **45**, 566 (1980).
[53] J. P. Perdew and A. Zunger, Phy. Rev. B **23**, 5048 (1981).
[54] D. Vanderbilt, Phys. Rev. B **41**, 7892 (1990).
[55] A. M. Rappe, K. M. Rabe, E. Kaxiras, and J. D. Joannopoulos, Phys. Rev. B **41**, 1227 (1990).
[56] See La pseudopotential file in https://www.physics.rutgers.edu/gbrv/.
[57] See In, Pb, and Bi pseudopotential files in http://theossrv1.epfl.ch/Main/Pseudopotentials and http://www.quantum-espresso.org/pseudopotentials/.
[58] W. Kohn and L. J. Sham, Phys. Rev. **140**, A1133 (1965).
[59] H. J. Monkhorst and J. D. Pack, Phys. Rev. B **13**, 5188 (1976).
[60] M. J. Mehl, J. E. Osburn, D. A. Papaconstantopoulos, and B. M. Klein, Phys. Rev. B **41**, 10311 (1990).
[61] M. J. Mehl, Phys. Rev. B **47**, 2493 (1993).
[62] F. D. Murnaghan, Proc. Natl. Acad. Sci. USA **30**, 224 (1944).
[63] W. Voigt, *Lehrbuch der Kristallphysik*, Leipzig, Taubner (1928).
[64] A. Reuss, Z. Angew. Math. Mech. **9**, 49 (1929).
[65] R. Hill, Proc., Phys. Soc. London A **65**, 349 (1952).
[66] O. L. Anderson, J. Phys. Chem. Solids **24**, 909 (1963).
[67] M. Born and K. Huang, *Dynamical Theory of Crystal Lattices* (Clarendon, Oxford, 1956).
[68] F. Pugh, Philos. Mag. **45**, 823 (1954).
[69] J. Haines, J. M. Leger, and G. Bocquillon, Annu. Rev. Mater. Res. **31**, 1 (2001).
[70] S. Ganeshan, S. L. Shang, H. Zhang, Y. Wang, M. Mantina, and Z. K. Liu, Intermetallics **17**, 313 (2009).